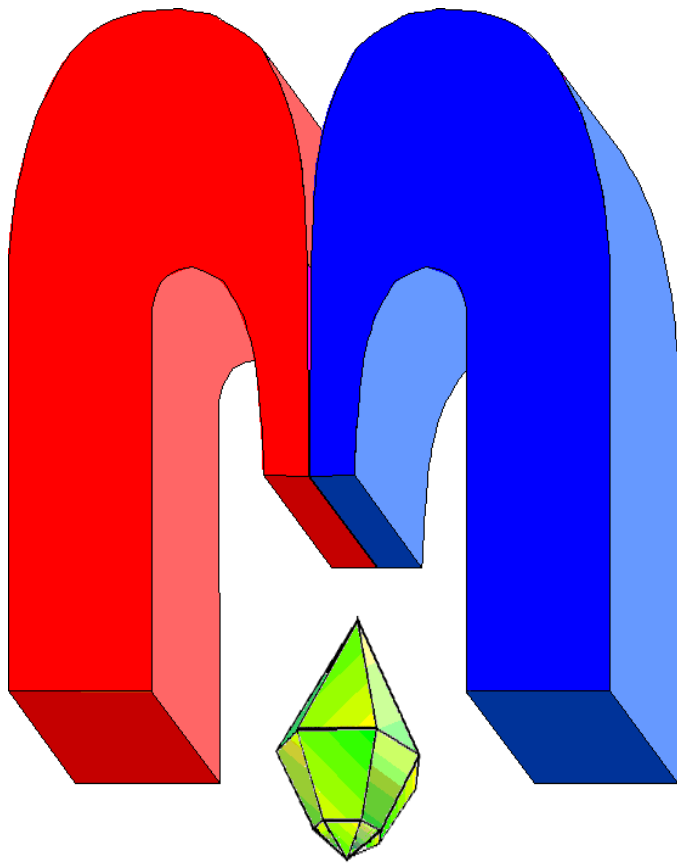


ISSN 2072-5981
doi: 10.26907/mrsej



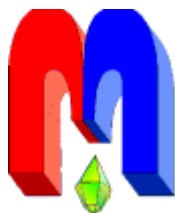
***magnetic
Resonance
in Solids***

Electronic Journal

*Volume 21
Special Issue 3
Paper No 19305
1-9 pages
2019*

doi: 10.26907/mrsej-19305

<http://mrsej.kpfu.ru>
<http://mrsej.ksu.ru>



Established and published by Kazan University
Endorsed by International Society of Magnetic Resonance (ISMAR)
Registered by Russian Federation Committee on Press (#015140),
August 2, 1996
First Issue appeared on July 25, 1997

© Kazan Federal University (KFU)*

"Magnetic Resonance in Solids. Electronic Journal" (MRSej) is a peer-reviewed, all electronic journal, publishing articles which meet the highest standards of scientific quality in the field of basic research of a magnetic resonance in solids and related phenomena.

Indexed and abstracted by
Web of Science (ESCI, Clarivate Analytics, from 2015), Scopus (Elsevier, from 2012), RusIndexSC (eLibrary, from 2006), Google Scholar, DOAJ, ROAD, CyberLeninka (from 2006), SCImago Journal & Country Rank, etc.

Editor-in-Chief

Boris **Kochelaev** (KFU, Kazan)

Honorary Editors

Jean **Jeener** (Universite Libre de Bruxelles, Brussels)

Raymond **Orbach** (University of California, Riverside)

Executive Editor

Yurii **Proshin** (KFU, Kazan)
mrsej@kpfu.ru



This work is licensed under a [Creative Commons Attribution-ShareAlike 4.0 International License](https://creativecommons.org/licenses/by-sa/4.0/).

 This is an open access journal which means that all content is freely available without charge to the user or his/her institution. This is in accordance with the [BOAI definition of open access](https://www.boai.ru/).

Editors

Vadim **Atsarkin** (Institute of Radio Engineering and Electronics, Moscow)

Yurij **Bunkov** (CNRS, Grenoble)

Mikhail **Eremin** (KFU, Kazan)

David **Fushman** (University of Maryland, College Park)

Hugo **Keller** (University of Zürich, Zürich)

Yoshio **Kitaoka** (Osaka University, Osaka)

Boris **Malkin** (KFU, Kazan)

Alexander **Shengelaya** (Tbilisi State University, Tbilisi)

Jörg **Sichelschmidt** (Max Planck Institute for Chemical Physics of Solids, Dresden)

Haruhiko **Suzuki** (Kanazawa University, Kanazava)

Murat **Tagirov** (KFU, Kazan)

Dmitrii **Tayurskii** (KFU, Kazan)

Valentine **Zhikharev** (KNRTU, Kazan)

Technical Editors of Issue

Maxim **Avdeev** (KFU)

Alexander **Kutuzov** (KFU)

* In Kazan University the Electron Paramagnetic Resonance (EPR) was discovered by Zavoisky E.K. in 1944.

Fluctuations of various order parameters in cuprate and Fe-based superconductors as revealed by microwave absorption measurements

I.I. Gimazov^{1,*}, Yu.I. Talanov¹, T. Adachi², T. Noji³, Y. Koike³, K. Omori³,
Y. Tanabe^{3,4}, D. Chareev^{5,6}, A. Vasiliev^{6,7}

¹Zavoisky Physical-Technical Institute, Kazan 420029, Russia

²Department of Engineering and Applied Sciences, Sophia University, Tokyo 102-8554, Japan

³Department of Applied Physics, Tohoku University, Sendai 980-8579, Japan

⁴Department of Physics, Tohoku University, Sendai 980-8578, Japan

⁵Institute of Experimental Mineralogy, RAS, Chernogolovka 142432, Russia

⁶Ural Federal University, Ekaterinburg 620002, Russia

⁷M.V. Lomonosov Moscow State University, Moscow 119991, Russia

*E-mail: gimazov@kfti.knc.ru

(Received March 10, 2019; accepted March 12, 2019; published April 19, 2019)

Fluctuations of various order parameters are considered as the significant components of understanding the mechanism of high- T_c superconductivity. To study these fluctuations in the cuprate and Fe-based superconductors we use the joint measurements of direct current resistivity and non-resonant microwave absorption. Comparing data obtained with both methods allowed us to extract the contribution of dynamic charge density waves in $\text{La}_{2-x}\text{Sr}_x\text{CuO}_4$, superconducting fluctuations in $\text{Bi}_2\text{Sr}_2\text{Ca}_{1-x}\text{Y}_x\text{Cu}_2\text{O}_8$ and nematic fluctuations in $\text{FeTe}_{1-x}\text{Se}_x$.

PACS: 74.40.+k, 74.70.-b, 74.72.-h, 52.70.Gw.

Keywords: high temperature superconductors, superconducting order parameter fluctuations, non-resonant microwave absorption.

*Dedicated to Boris I. Kochelaev, mentor and colleague,
on the occasion of his 85th birthday*

1. Introduction

The search of key interaction responsible for the Cooper pair formation in cuprate and Fe-based superconductors is associated with the necessary study of the numerous phases being above the superconducting transition temperature T_c . The order parameters of these phases are of different nature: magnetic, orbital, charge *et al.* All of them are to some extent under suspicion of responsibility for the electron pairing. In other words, the fluctuations of one of these order parameters could be “a glue of Cooper pairs”. The most preferred candidates for this role are magnetic fluctuations (or correlations). There is much speculation that the antiferromagnetic correlations of spin-density-wave (SDW) type are responsible for the electron scattering above T_c , and for their pairing below T_c , and for the rotational symmetry breaking (that is for nematic ordering) as well (see, *e. g.*, [1–4]). For this reason the spin fluctuations are intensively investigated with the neutron scattering and other methods in cuprate superconductors [1, 2, 5, 6], iron pnictides [3, 4, 7–9] and iron chalcogenides [10–13]. Note, there are other applicants for the role of the Cooper pairs glue except spin fluctuations. Among them are the Jahn-Teller-type electron-lattice interaction [14] nematic fluctuations [15] *etc.*

The fluctuation impact on the electron scattering can be found upon applying a hydrostatic pressure and/or a high magnetic field. In this case their influence is manifested via the change

of the resistivity versus temperature dependence [16, 17]. This is because of the fluctuation strengthening at high pressure. At the ambient pressure the fluctuations are weak and short-lived, their lifetime is shorter than the electron-scattering time τ . Therefore, their impact on the DC resistivity is negligible. Then they can be detected with the high-frequency measurements only. As an example, the optical pump-probe study has revealed the long-lived long-range nematic order at temperatures below the structural tetragonal-to-orthorhombic transition T_s and short-lived ($\sim 10^{-12}$ s) fluctuations at $T > T_s$ [15]. And the terahertz spectroscopy allowed the authors of Ref. [18] to detect the superconducting fluctuation (SCF) at temperatures a few degrees higher than T_c . The data presented in this article was obtained with the nonresonant microwave absorption (MWA) measurements at frequency 9.2 GHz on various cuprate and Fe chalcogenide superconductors. It accumulates results of study performed on crystals $\text{La}_{2-x}\text{Sr}_x\text{CuO}_4$, $\text{Bi}_2\text{Sr}_2\text{Ca}_{1-x}\text{Y}_x\text{Cu}_2\text{O}_{8+y}$ and $\text{FeTe}_{1-x}\text{Se}_x$ and published previously [19–21].

MWA is determined by the current carrier scattering, and so the comparison of the MWA data obtained at the frequency of the order of $\sim 10^{10}$ Hz with the DC resistivity data allows us to separate the contribution of the short-lived excitations (such as fluctuations of different type, dynamical charge density wave and so on) to the ohmic loss.

2. Measurement technique

In a conductive material the microwave absorption takes place in a skin-layer. Therefore, the MWA value is proportional to the skin-layer volume. The temperature variation of the skin-layer thickness leads to the dependence of the MWA signal amplitude on temperature $A_{\text{MWA}}(T)$. The skin-layer thickness is determined by the resistivity ρ as $\delta = c(\rho/2\pi\omega\mu)^{1/2}$ (c is the light speed, ω is the frequency, and μ is the magnetic permeability). Thus $A_{\text{MWA}} \propto \sqrt{\rho}$. The ohmic loss is the main contribution to microwave absorption. The contributions due to the fluctuations of various order parameters can be separated by comparing the functions $A_{\text{MWA}}(T)$ and $\sqrt{\rho(T)}$.

The microwave absorption of sample studied was measured using the standard electron spin resonance (ESR) spectrometer Bruker BER-418s. Its working frequency is $9.2 \div 9.5$ GHz. The spectrometer is sensitive to the weak short-lived electron excitations owing to the lock-in technique of the signal detection and amplification with 100 kHz magnetic modulation. To keep the applied magnetic field to be constant during the measurement, we replaced the applied field modulation by the modulation of the incident microwave radiation. The microwave field modulation is realized with the PIN-diode inserted in the waveguide between a clystron (the microwave radiation source) and the cavity resonator of TE_{102} mode with a sample placed into its center. The temperature variation performed with the helium-gas-flow cryostat in the range from a room temperature down to 7 K.

The sample resistance was measured using a standard four-probe method at the direct current 3.6 mA. The superconducting transition is determined via the magnetic AC susceptibility measurements at a frequency 1.3 kHz.

3. Results and discussion

3.1. Superconducting fluctuations in $\text{Bi}_2\text{Sr}_2\text{Ca}_{1-x}\text{Y}_x\text{Cu}_2\text{O}_{8+y}$

The $\text{Bi}_2\text{Sr}_2\text{CaCu}_2\text{O}_8$ compound has a pronounced layered structure of the crystal lattice. In many cases it behaves like quasi-two-dimensional system. For this reason, fluctuations manifest themselves in many phenomena taking place in this material. In particular, superconducting fluctuations (SCF) have a noticeable effect on the diamagnetic response [22, 23], the Nernst sig-

nal [24] in the temperature range as wide as several tens of degrees Kelvin. We have found the SCF influence on the MWA in the $\text{Bi}_2\text{Sr}_2\text{Ca}_{1-x}\text{Y}_x\text{Cu}_2\text{O}_{8+y}$ crystals [20].

The crystals with various current carrier (holes) density were studied. To change the hole density in samples, calcium was partially substituted for yttrium in the $\text{Bi}_2\text{Sr}_2\text{CaCu}_2\text{O}_8$ compound. Varying Y concentrations x in $\text{Bi}_2\text{Sr}_2\text{Ca}_{1-x}\text{Y}_x\text{Cu}_2\text{O}_8$ from 0 to 0.2, samples with different doping are obtained: at $x = 0$ a sample is overdoped by holes (OD) and has $T_c = 88$ K; at $x = 0.1$ a sample is optimally doped (OP) with $T_c = 94$ K; when $x = 0.2$ a sample is underdoped (UD) with $T_c = 77$ K.

The variation of the MWA amplitude A_{MWA} with temperature is shown in Fig.1 for three samples. It decreases slightly with lowering the temperature from 300 K down to some temperature T_f marked with a vertical arrow in the figure. Below this temperature the $A_{\text{MWA}}(T)$ dependence slope changes a sign. An upturn of the $A_{\text{MWA}}(T)$ function at $T = T_f$ is found for OP and UD samples, but not for OD. The sharp decrease of A_{MWA} at superconducting transition is observed in all samples. Note, the metallic character of the $A_{\text{MWA}}(T)$ dependence at $T > T_f$ corresponds to the $\rho(T)$ dependence. However, the latter does not demonstrate an upturn in the whole temperature range down to T_c . Therefore, one can conclude that some short-lived excitations contribute to MWA but not to resistivity.

The maximum of the $A_{\text{MWA}}(T)$ dependence near the critical temperature is called “loss peak”. Its origin is discussed in Ref. [25] on the basis of the theoretical work [26]. In line with the model of [25] the appearance of the loss peak is governed by the superconducting fluctuations formed in a sample at the temperature close T_c . We trace the emergence of the MWA temperature dependence anomaly caused by SCF T_f marked by arrows in Fig.1. The MWA amplitude versus T was recorded for the $\text{Bi}_2\text{Sr}_2\text{Ca}_{1-x}\text{Y}_x\text{Cu}_2\text{O}_8$ crystals with various x . The loss peak due to SCF is observed on $A_{\text{MWA}}(T)$ dependence of all samples except for OD. We assume T_f is very close to T_c for this sample.

The obtained T_f dependence on the hole density p was plotted on the “temperature – hole density” phase diagram along with the critical temperature $T_c(p)$ and the pseudo gap temper-

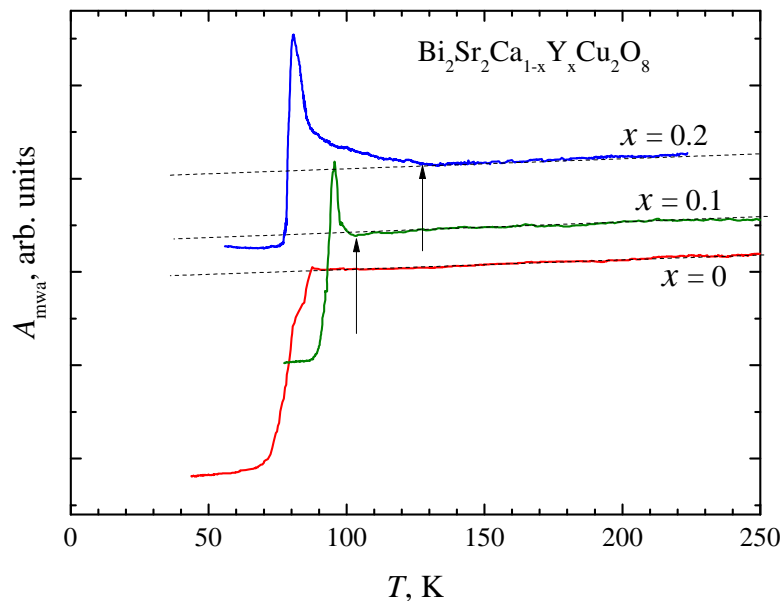


Figure 1. Temperature dependence of the MWA signal amplitude for the $\text{Bi}_2\text{Sr}_2\text{Ca}_{1-x}\text{Y}_x\text{Cu}_2\text{O}_{8+y}$ with various Y doping.

ature $T^*(p)$. The phase diagram has adduced in our early work [20]. The $T_f(p)$ dependence determines the upper boundary of the fluctuation area as revealed by the MWA measurements. $T_c(p)$ is its lower boundary. The obtained data indicates the presence of superconducting fluctuations in the wide temperature range for the underdoped samples. This range decreases as the hole density increases and becomes zero for the OD sample. This fact together with the absence of the loss peak in the pnictide data [20] gives the basis for the assumption on stimulating effect of the pseudogap on the SCF development. The SCF detection using the MWA technique indicates the fluctuation lifetime on order of 10^{-10} s or more. Our estimates of $T_f(p)$ are in good agreement with the ARPES [27] and STS data [28] but diverge from the Nernst effect measurements [24] in the region of the large hole density.

3.2. Dynamic charge density waves in $\text{La}_{2-x}\text{Sr}_x\text{CuO}_4$

$\text{La}_{2-x}\text{Sr}_x\text{CuO}_4$ (LSCO) is another famous member of the cuprate superconductor family. Fluctuations of the superconducting order parameter in this material were studied in detail by means of the diamagnetic response investigation [29] and the Nernst effect measurements [24]. The latter revealed a very wide temperature range of SCF, which amounts about 100 K at $x = 0.1$. However, the later works (see, *e. g.* [30]) casted doubt on the interpretation of the Nernst effect data [24] and estimated T_f being only ~ 20 K higher than T_c . Moreover, using THz time-domain spectroscopy to probe the superconducting fluctuations in $\text{La}_{2-x}\text{Sr}_x\text{CuO}_4$ thin films allowed the authors of [18] to conclude that they persist in a comparatively narrow temperature range, at most 16 K above T_c . The authors of [31] explained the Nernst signal at higher temperatures by the influence of the stripe order fluctuations. Thus, the stripe order plays a significant role at some temperature range. The dynamical forms of the stripe structure, such as spin density waves (SDW) and charge density waves (CDW), admix to SCF and complicate considerably understanding the picture. Dynamical CDW provide a high conductivity and metallic character of the resistivity versus temperature dependence $\rho(T)$ [32]. If there are obstacles for the CDW motion, the form of $\rho(T)$ changes drastically from the metallic type to the activation one. This occurs below the structural transition temperature T_s where the crystal structure turns from tetragonal form ($T > T_s$) to orthorhombic one ($T < T_s$) in compounds $\text{La}_{2-x}\text{Ba}_x\text{CuO}_4$ and $\text{La}_{2-x}\text{Sr}_x\text{CuO}_4$ doped with neodymium Nd. At $T < T_s$ CDW's become pinned. It produces a condition of weak localization of current carriers and the $\rho(T)$ dependence character changes. There is no pinning structure in $\text{La}_{2-x}\text{Sr}_x\text{CuO}_4$ without Nd. CDWs have the dynamical or fluctuational nature here. To detect them the high-frequency technique is required, such as MWA measurements.

The $\text{La}_{2-x}\text{Sr}_x\text{CuO}_4$ single crystals studied in our work were grown with the traveling solvent floating zone techniques at the Tohoku University, Japan. The hole concentration per Cu ion (the hole density p) in this compound coincides with the strontium concentration x . It allows one to control the hole density by changing x . The optimally doped (OP) sample with $x = 0.16$ has the highest critical temperature $T_c = 37.6$ K. T_c of overdoped (OD) crystal is slightly lower (32.2 K), and the transition temperatures of several underdoped (UD) samples fall gradually with decreasing x down to 19.3 K at $x = 0.077$. The superconducting transition temperatures were determined with the AC susceptibility measurements as the onset of the diamagnetic response.

The temperature dependence of the MWA amplitude is shown in Fig. 2 for two UD and one OP LSCO samples. The deviation (upturn) is seen from the linear dependence upon decreasing the temperature below the certain point depicted by arrow in Fig. 2. The same deviation is observed for all underdoped samples but it is absent in OP and OD samples. In the last samples $A_{\text{MWA}}(T)$ decreases monotonically down to critical temperature where the sharp fall takes place.

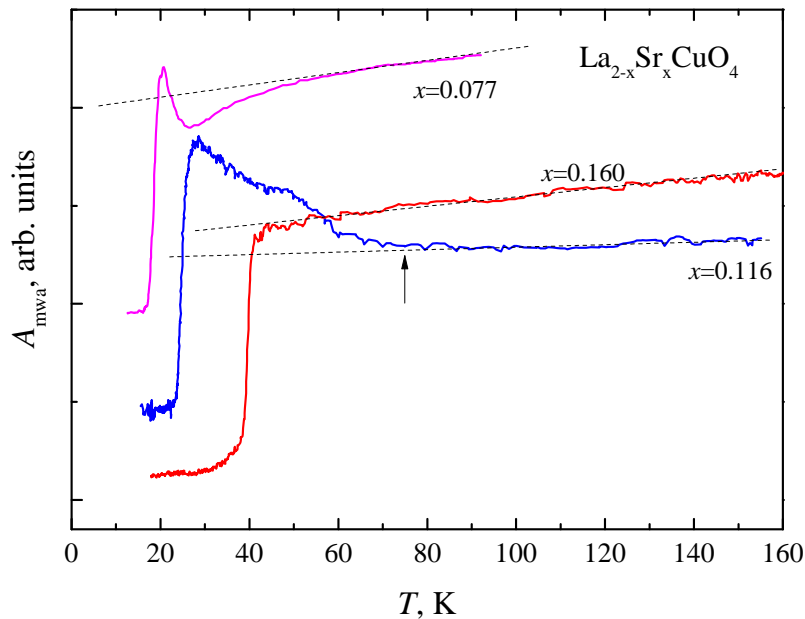


Figure 2. Temperature dependence of the MWA signal amplitude for the $\text{La}_{2-x}\text{Sr}_x\text{CuO}_4$ samples with various Sr concentration. The straight lines are drawn to easy find the deviation of $A_{\text{MWA}}(T)$ from the linear dependence.

The upturn of the $A_{\text{MWA}}(T)$ function is indicative of the emergence of the additional scattering channel with lowering temperature. It is possibly connected with fluctuating CDW. However, the superconducting fluctuations can contribute to MWA at temperatures close to T_c as well (see, *e. g.*, [20,25,26]). The impact of the magnetic field on the $A_{\text{MWA}}(T)$ dependence allows one to separate these two contributions. The MWA loss peak due to SCFs discussed in the previous paragraph is broadened and shifted with increasing field [26] while the CDW contribution is unaffected by magnetic field. For the UD sample with $x = 0.077$ and $T_c = 19.3$ K the upturn occurs at 27 K, while the field dependence arises below 24 K. Thus one can assume that the temperature of the CDW emergence T_{CDW} is 27 K. Another UD sample with $x = 0.116$ and $T_c = 24.3$ K demonstrates the upturn due to CDWs at 75 K (depicted by arrow in Fig. 2) and the field dependence below 43 K. Thus, the $A_{\text{MWA}}(T)$ curves obtained at various magnetic fields for the LSCO crystals with various x enable us to derive the boundary points of the regions with CDWs, superconducting fluctuations and the bulk superconductivity state. The $x - T$ phase diagram of the $\text{La}_{2-x}\text{Sr}_x\text{CuO}_4$ compound is plotted on the base of obtained data and presented in our work [19]. It was found that the doping range of the CDW presence in LSCO is considerably broader than that obtained from the XRD study [33]. This observation correlates well with the transport data [32].

3.3. Nematic fluctuations in $\text{FeTe}_{1-x}\text{Se}_x$

Fe-based superconductors have many properties similar to that of cuprates: layered structure, reach phase diagram and the influence of various order fluctuations on their characteristics. In iron pnictides the magnetic ordering of the SDW type and the nematic ordering take place simultaneously below the temperature of the tetra-ortho structural transition T_s while in iron chalcogenides the nematic order occurs without the magnetic state establishment. (The nematic ordering is characterized by breaking the fourfold rotational symmetry and by formation of the twofold symmetry of electronic parameters, such as resistivity, magnetic susceptibility etc.) This difference can be eliminated by applying a pressure [16]. At an ambient pressure the long-lived long-range nematic order exists only in a few of iron chalcogenide compounds (FeSe and

FeSe_{1-x}S_x) at $T < T_s$. And above T_s there are only fluctuations of nematic order parameter [15]. In the compound with partial substitution of Se by Te (FeTe_{1-x}Se_x) the structural transition does not occur. Therefore, the nematic order can be present in the form of fluctuations only. To detect them we use the MWA measurements again.

The crystals with the various Se/Te ratio were investigated. They were grown using the flux technique. The sample composition obtained with the energy-dispersive X-ray spectroscopy (EDX) revealed excess iron in all samples except for pure FeSe. The last sample has a narrow superconducting transition with $T_c^{\text{onset}} = 9.1$ K while the transition is broad in FeTe_{1-x}Se_x with $T_c^{\text{onset}} = 12 \div 15$ K depending on a sample composition. The broad transition testifies about the sample heterogeneity, which is consequence of an excess iron.

The comparison of the MWA versus temperature data with the resistivity measurements is shown in Fig.3 for FeSe. In this figure and hereafter the resistivity data are plotted as square root of ρ . Such comparison takes into account the circumstance that $A_{\text{MWA}} \propto \sqrt{\rho}$ in normal state without fluctuations (see Part 2). The temperature variation of the resistivity has all features described in literature (see, *e. g.*, [15,16]). It has the positive slope over the whole region above T_c and the anomaly near $T_s \simeq 90$ K due to the tetragonal to orthorhombic structural transition. ρ falls sharply down to zero at the superconducting transition $T_c \simeq 9$ K. In Fig. 3 the MWA amplitude value is attached to the $\sqrt{\rho}$ data by magnitude and slope at high temperatures. The $A_{\text{MWA}}(T)$ function has all features listed above for the $\sqrt{\rho(T)}$ dependence. However the magnitudes of two function diverge in the temperature range from T_c to ~ 170 K. We suggest the discrepancy is due to the short-lived fluctuations of spin or nematic order. They contribute to MWA, but not to the DC resistivity because of their life-time shorter than the electron scattering time.

The divergence between two functions increases with the temperature decrease and reaches its maximum just below T_s . With further lowering the temperature the divergence diminishes and becomes negligible close to T_c . The similar behavior was found for the nematic-order contribution to the in-plane resistivity anisotropy of the FeSe crystal [34]. This gives grounds for conclusion that the additional contribution to MWA is due precisely to nematic fluctuations.

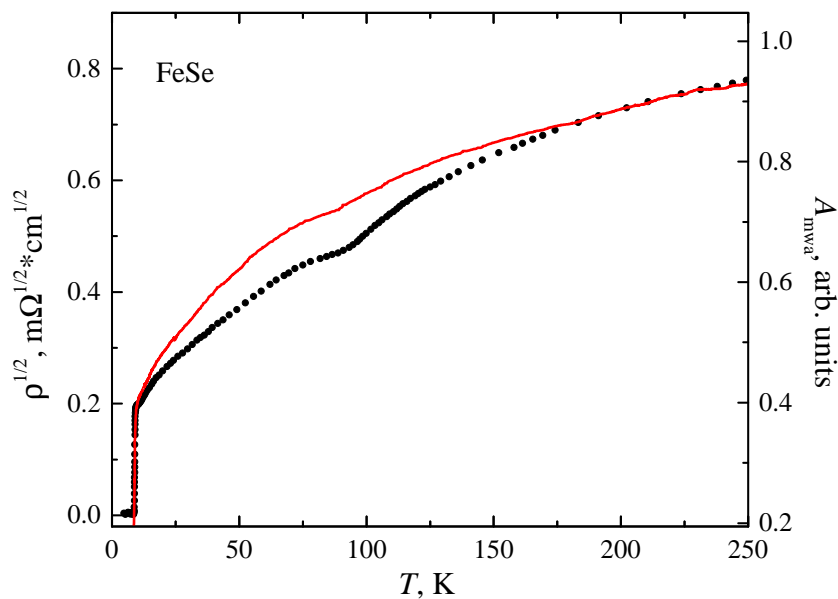


Figure 3. Temperature dependence of the $\rho^{1/2}$ (points) and the A_{MWA} (line) for the FeSe sample.

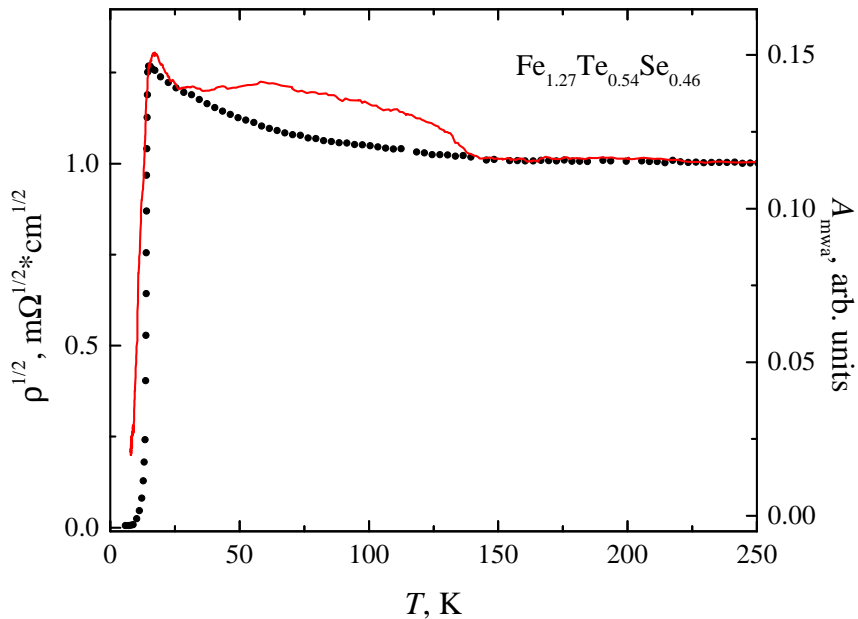


Figure 4. Temperature dependence of the $\rho^{1/2}$ (points) and the A_{MWA} (line) for the $\text{Fe}_{1.27}\text{Te}_{0.54}\text{Se}_{0.46}$ sample.

The consequences of the partial substitution of Se by Te in the FeSe compound can be traced on the example of the $\text{Fe}_{1+y}\text{Te}_{1-x}\text{Se}_x$ crystal with the approximately equal Te and Se portions: $\text{Fe}_{1.27}\text{Te}_{0.54}\text{Se}_{0.46}$. The Te addition results in the excess iron appearance. It induces the weak localization effect which manifests as the activation form of resistivity $\rho(T)$ at temperatures above T_c (see Fig. 4). There is no anomaly due to the tetra-ortho structural transition on the $\rho(T)$ dependence and, as a consequence, the long-range nematic order does not emerge. However, the comparison of the $A_{MWA}(T)$ and $\rho(T)$ functions in Fig. 4 shows the fluctuation contribution to MWA in the range from 30 K to 140 K. Since $\text{Fe}_{1.27}\text{Te}_{0.54}\text{Se}_{0.46}$ and FeSe are akin compounds, the probability of the nematic nature of the fluctuations is high enough.

The results of the comparative study of the DC resistivity and microwave absorption in the $\text{Fe}_{1+y}\text{Te}_{1-x}\text{Se}_x$ crystals are in good agreement with the neutron scattering study of spin fluctuations in such samples [10]. The neutron study showed the presence and competition of two types of magnetic correlations (*i. e.*, fluctuations): isotropic (Neel) type and anisotropic (stripe) type. The latter most likely might be an origin of the nematic fluctuation observed in our study. More detailed discussion of the results obtained on the $\text{Fe}_{1+y}\text{Te}_{1-x}\text{Se}_x$ samples is published in the work [21].

In conclusion, the comparative analysis of the resistivity data and the microwave absorption results gives the unique opportunity to separate the contribution of short-lived excitations, in particular the superconducting fluctuations, the dynamical charge density waves and the nematic fluctuations in cuprate and Fe-based superconductors.

Acknowledgments

This work was supported by the Russian Academy of Sciences via the grant of Program 1.12 “Fundamental Problems of High-Temperature Superconductivity”. The work of D.Ch. is supported by the program 211 of the Russian Federation Government, agreement No. 02.A03.21.0006 and by the Russian Government Program of Competitive Growth of Kazan Federal University. The work of A.V. has been supported by Act 211 of the Government of Russian Federation, Contracts No. 02.A03.21.0006 and No. 02.A03.21.0011.

References

1. Wilson S.D., Dai P., Li S., Chi S., Kang H.J., Lynn J.W. *Nature* **442**, 59 (2006)
2. Taillefer L. *Ann. Rev. Cond. Mat. Phys.* **1**, 51 (2010)
3. Kim M.G., Lamsal J., Heitmann T.W., Tucker G.S., Pratt D.K., Khan S.N., Lee Y.B., Alam A., Thaler A., Ni N., Ran S., Bud'ko S.L., Marty K.J., Lumsden M.D., Canfield P.C., Harmon B.N., Johnson D.D., Kreyssig A., McQueeney R.J., Goldman A.I. *Phys. Rev. Lett.* **109**, 167003 (2012)
4. Dioguardi A.P., Lawson M.M., Bush B.T., Crocker J., Shirer K.R., Nisson D.M., Kissikov T., Ran S., Bud'ko S.L., Canfield P.C., Yuan S., Kuhns P.L., Reyes A.P., Grafe H.-J., Curro N.J. *Phys. Rev. B* **92**, 165116 (2015)
5. Hayden S.M., Mook H.A., Dai P., Perring T.G., Dogan F. *Nature* **429**, 531 (2004)
6. Tranquada J.M., Woo H., Perring T.G., Goka H., Gu G.D., Xu G., Fujita M., Yamada K. *Nature* **429**, 534 (2004)
7. Inosov D.S., Park J.T., Bourges P., Sun D.L., Sidis Y., Schneidewind A., Hradil K., Haug D., Lin C.T., Keimer B., Hinkov V. *Nat. Phys.* **6**, 178 (2009)
8. Parshall D., Lokshin K.A., Niedziela J., Christianson A.D., Lumsden M.D., Mook H.A., Nagler S.E., McGuire M.A., Stone M.B., Abernathy D.L., Sefat A.S., Sales B.C., Mandrus D.G., Egami T. *Phys. Rev. B* **80**, 012502 (2009)
9. Lester C., Chu J.-H., Analytis J.G., Perring T.G., Fisher I.R., Hayden S.M. *Phys. Rev. B* **80**, 064505 (2010)
10. Liu T.J., Hu J., Qian B., Fobes D., Mao Z.Q., Bao W., Reehuis M., Kimber S.A.J., Prokeš K., Matas S., Argyriou D.N., Hiess A., Rotaru A., Pham H., Spinu L., Qiu Y., Thampy V., Savici A.T., Rodriguez J.A., Broholm C. *Nature Materials* **9**, 716 (2010)
11. Xu Z., Wen V., Xu G., Chi S., Ku W., Gu G., Tranquada J.M. *Phys. Rev. B* **84**, 052506 (2011)
12. Wang Q., Shen Y., Pan B., Zhang X., Ikeuchi K., Iida K., Christianson A.D., Walker H.C., Adroja D.T., Abdel-Hafiez M., Chen X., Chareev D.A., Vasiliev A.N., Zhao J. *Nat. Commun.* **7**, 12182 (2016)
13. Imai T., Ahilan K., Ning F.L., McQueen T.M., Cava R.J. *Phys. Rev. Lett.* **102**, 177005 (2009)
14. Keller H., Bussmann-Holder A., Müller K.A. *Materials Today* **11**, 38 (2008)
15. Luo C.-W., Cheng P.C., Wang S.-H., Chiang J.-C., Lin J.-Y., Wu K.-H., Juang J.-Y., Chareev D.A., Volkova O.S., Vasiliev A.N. *npj Quantum Materials* **2**, 32 (2017)
16. Terashima T., Kikugawa N., Kasahara S., Watashige T., Matsuda Y., Shibauchi T., Uji S. *Phys. Rev. B* **93**, 180503(R) (2016)
17. Kang J.-H., Jung S.-G., Lee S., Park E., Lin J.-Y., Chareev D.A., Vasiliev A.N., Park T. *Supercond. Sci. Technol.* **29**, 035007 (2016)
18. Bilbro L.S., Aguilar R.V., Logvenov G., Pelleg O., Bozovic I., Armitage N.P. *Nat. Phys.* **7**, 298 (2011)

19. Gimazov I.I., Adachi T., Omori K., Tanabe Y., Koike Y., Talanov Yu.I. *JETP Lett.* **108**, 675 (2018)
20. Gimazov I., Talanov Yu., Sakhin V., Adachi T., Noji T., Koike Y. *Appl. Magn. Reson.* **48**, 861 (2017)
21. Gimazov I.I., Lyadov N.M., Chareev D.A., Vasiliev A.N., Talanov Yu.I. *JETP* **155**, 6 (2019)
22. Li L., Wang Y., Naughton M.J., Ono S., Ando Y., Ong N.P. *Europhys. Lett.* **72**, 451 (2005)
23. Wang Y., Li L., Naughton M.J., Gu G.D., Uchida S., Ong N.P. *Phys. Rev. Lett.* **95**, 247002 (2005)
24. Wang Y., Li L., Ong N.P. *Phys. Rev. B* **73**, 024510 (2006)
25. Grbić M.S., Barišić N., Dulčić A., Kupčić I., Li Y., Zhao X., Yu G., Dressel M., Greven M., Požek M. *Phys. Rev. B* **80**, 094511 (2009)
26. Gough C.E., Exon N.J. *Phys. Rev. B* **50**, 488 (1994)
27. Zhang W., Smallwood C.L., Jozwiak C., Miller T.L., Yoshida Y., Eisaki H., Lee D.-H., Lanzara A. *Phys. Rev. B* **88**, 245132 (2013)
28. Gomes K.K., Pasupathy A.N., Pushp A., Ono S., Ando Y., Yazdan Y. *Nature* **447**, 569 (2007)
29. Carballeira C., Mosqueira J., Revcolevschi A., Vidal F. *Physica C* **384**, 185 (2003)
30. Cyr-Choiniere O., Daou R., Laliberte F., Collignon C., Badoux S., LeBoeuf D., Chang J., Ramshaw B.J., Bonn D.A., Hardy W.N., Liang R., Yan J.-Q., Cheng J.-G., Zhou J.-S., Goodenough J.B., Pyon S., Takayama T., Takagi H., Doiron-Leyraud N., Taillefer L. *Phys. Rev. B* **97**, 064502 (2018)
31. Cyr-Choiniere O., Daou R., Laliberte F., LeBoeuf D., Doiron-Leyraud N., Chang J., Yan J.-Q., Cheng J.-G., Zhou J.-S., Goodenough J.B., Pyon S., Takayama T., Takagi H., Tanaka Y., Taillefer L. *Nature* **458**, 743 (2009)
32. Ando Y., Lavrov A.N., Komiya S., Segawa K., Sun X.F. *Phys. Rev. Lett.* **87**, 017001 (2001)
33. Christensen N.B., Chang J., Larsen J., Fujita M., Oda M., Ido M., Momono N., Forgan E.M., Holmes A.T., Mesot J., Huecker M., Zimmermann M.V. [arXiv:1404.3192](https://arxiv.org/abs/1404.3192) (2014)
34. Tanatar M.A., Böhmer A.E., Timmons E.I., Schütt M., Drachuck G., Taufour V., Kothapalli K., Kreyssig A., Bud'ko S.L., Canfield P.C., Fernandes R.M., Prozorov R. *Phys. Rev. Lett.* **117**, 127001 (2016)